

University of Nebraska - Lincoln DigitalCommons@University of Nebraska - Lincoln

Faculty Publications from Nebraska Center for
Materials and Nanoscience

Materials and Nanoscience, Nebraska Center for
(NCMN)

2016

Modification of the G-phonon mode of graphene by nitrogen doping

Pavel V. Lukashev

University of Northern Iowa, pavel.lukashev@uni.edu

Liuyan Zhao

Columbia University, lyzhao@umich.edu

Tula R. Paudel

University of Nebraska-Lincoln, tula.paudel@gmail.com

Theanne Schiros


Columbia University

Noah Hurley

University of Northern Iowa

See next page for additional authors

Follow this and additional works at: <http://digitalcommons.unl.edu/cmrafacpub>

 Part of the [Atomic, Molecular and Optical Physics Commons](#), [Condensed Matter Physics Commons](#), [Engineering Physics Commons](#), and the [Other Physics Commons](#)

Lukashev, Pavel V.; Zhao, Liuyan; Paudel, Tula R.; Schiros, Theanne; Hurley, Noah; Tsymbal, Evgeny Y.; Pinczuk, Aron; Pasupathy, Abhay; and He, Rui, "Modification of the G-phonon mode of graphene by nitrogen doping" (2016). *Faculty Publications from Nebraska Center for Materials and Nanoscience*. 118.

<http://digitalcommons.unl.edu/cmrafacpub/118>

This Article is brought to you for free and open access by the Materials and Nanoscience, Nebraska Center for (NCMN) at DigitalCommons@University of Nebraska - Lincoln. It has been accepted for inclusion in Faculty Publications from Nebraska Center for Materials and Nanoscience by an authorized administrator of DigitalCommons@University of Nebraska - Lincoln.

Authors

Pavel V. Lukashev, Liuyan Zhao, Tula R. Paudel, Theanne Schiros, Noah Hurley, Evgeny Y. Tsymbal, Aron Pinczuk, Abhay Pasupathy, and Rui He



Modification of the G-phonon mode of graphene by nitrogen doping

Pavel V. Lukashev,^{1,a)} Liuyan Zhao,² Tula R. Paudel,³ Theanne Schiros,^{4,5} Noah Hurley,¹ Evgeny Y. Tsybmal,³ Aron Pinczuk,^{2,6} Abhay Pasupathy,² and Rui He^{1,2,b)}

¹Department of Physics, University of Northern Iowa, Cedar Falls, Iowa 50614, USA

²Department of Physics, Columbia University, New York, New York 10027, USA

³Department of Physics and Astronomy and Nebraska Center for Materials and Nanoscience, University of Nebraska, Lincoln, Nebraska 68588, USA

⁴Materials Research Science and Engineering Center, Columbia University, New York, NY 10027, USA

⁵Department of Science and Mathematics, Fashion Institute of Technology, New York, NY 10001, USA

⁶Department of Applied Physics and Applied Mathematics, Columbia University, New York, New York 10027, USA

(Received 2 November 2015; accepted 15 January 2016; published online 27 January 2016)

The effect of nitrogen doping on the phonon spectra of graphene is analyzed. In particular, we employ first-principles calculations and scanning Raman analysis to investigate the dependence of phonon frequencies in graphene on the concentration of nitrogen dopants. We demonstrate that the G phonon frequency shows oscillatory behavior as a function of nitrogen concentration. We analyze different mechanisms which could potentially be responsible for this behavior, such as Friedel charge oscillations around the localized nitrogen impurity atom, the bond length change between nitrogen impurity and its nearest neighbor carbon atoms, and the long-range interactions of the nitrogen point defects. We show that the bond length change and the long range interaction of point defects are possible mechanisms responsible for the oscillatory behavior of the G frequency as a function of nitrogen concentration. At the same time, Friedel charge oscillations are unlikely to contribute to this behavior. © 2016 AIP Publishing LLC. [<http://dx.doi.org/10.1063/1.4940910>]

Ever increasing interest in graphene in recent years is due to the peculiar and unique properties of this material, such as thermal conductivity,^{1,2} mechanical strength,^{3,4} and electrical⁵ and optical⁶ conductivities. The possibility to tune these properties by chemical modification has recently attracted significant attention.^{7–10} Different properties of graphene could be modulated and enhanced by doping, thermal treatment, external pressure, etc. For example, it has been recently suggested that doping of graphene with electron-donor nitrogen can produce an *n*-type semiconductor.^{9,11} Different practical applications of these modulations have been suggested, such as field-effect transistors,^{12–14} anodes of lithium-ion batteries,¹⁵ and ferroelectric tunnel junctions.¹⁶ Naturally, these and similar findings challenge researchers and engineers to optimize the properties of graphene for industry ready applications. In general, it is expected that doping induced judicious tuning of electronic, optical, and mechanical properties of graphene could potentially result in its integration in nanoelectronic circuits of the near future.

Significant progress has been achieved recently in describing the atomic structure of doped graphene at the microscopic level.^{11,17} Two stable configurations of graphene doping are usually considered—pyridine-like and substitution doping.^{8,11} In the former, three two-coordinated dopant atoms surround a vacancy site, while in the latter dopant atoms replace carbon atoms. Depending on the dopant, both *n*- and *p*-type dopings occur. The underlying geometry of doping is typically studied with scanning tunneling microscopy (STM) and/or density functional theory (DFT) calculations. However, despite significant progress, it is still unclear how the underlying geometry

and lattice vibrations depend on the concentration of dopant. From a computational perspective, such analysis is challenging, since for the realistic simulations, it requires structure optimizations and calculations of phonon spectra for large supercells of up to a few hundred atoms. From an experimental viewpoint, systematic analysis of the lattice geometry (i.e., interatomic distances) through the spectroscopy techniques is also challenging. In this paper, we address these issues from both computational and experimental angles. In particular, we show that the phonon G-mode frequency shifts exhibit oscillatory behavior as a function of nitrogen concentration. The unit cell of graphene consists of two atoms; hence, there are six normal modes at the Brillouin zone center Γ : $A_{2u} + B_{2g} + E_{1u} + E_{2g}$ (E_{1u} and E_{2g} are doubly degenerate). E_{1u} and A_{2u} are acoustic modes corresponding to translations parallel and perpendicular to the graphene plane. E_{2g} and B_{2g} are optical modes corresponding to out-of-phase movement of carbon atoms in the two sublattices. While the B_{2g} mode is both infrared and Raman inactive, the E_{2g} mode is Raman active and is often known as the G-mode. We analyze mechanisms which could potentially be responsible for the oscillatory behavior of the phonon G-mode frequency as a function of nitrogen concentration, such as Friedel oscillations around charge impurities, the N-C bond length change, and the long range interactions between nitrogen point defects.

The paper is organized as follows: first we describe used computational and experimental techniques; then we outline our main experimental results on the phonon G-frequency shifts; next, we present theoretical analysis and discussions; and finally we present some concluding remarks.

In this study, we have performed Raman spectroscopy measurements on Chemical Vapor Deposition (CVD) grown Nitrogen-doped (N-doped) monolayer graphene films with

a) pavel.lukashev@uni.edu

b) rui.he@uni.edu

multiple N doping levels. The graphene films were synthesized on copper foil substrates in a quartz tube furnace.^{10,11} The foil substrate was precleaned with a flow of 10 sccm H₂ at a pressure of ~ 0.055 Torr and a temperature of 1000 °C for 10 min. Following this, mixtures of CH₄ (170 sccm), H₂ (10 sccm), and NH₃ with a tunable pressure ratio of CH₄:NH₃ were introduced in the furnace at a total pressure of 1.9–2.2 Torr and kept at a temperature of 1000 °C for 18 min. The samples used in this study include four CH₄:NH₃ ratios of 4:170, 7:170, 10:170, and 13:170. Due to the fact that copper typically contributes strong luminescence in optical measurements, we transferred the as-grown N-doped graphene films onto SiO₂/Si substrates for Raman measurements. The as-grown graphene films were first coated with a layer of 200 nm thick PMMA, and then, the copper foil substrate was dissolved in FeCl₃ (20 wt. %) solution. The PMMA/graphene layer was rinsed in deionized water multiple times before it was transferred onto the SiO₂/Si substrate. Finally, PMMA was dissolved in acetone with a graphene layer left on the SiO₂/Si substrate. Raman spectra were taken on transferred N-doped graphene samples using a Renishaw inVia Raman microscope with a laser wavelength of 532 nm. The spectral resolution is ~ 1.4 cm⁻¹. The laser was focused using a 100 \times objective lens (numerical aperture 0.85), which gave a laser spot size (diameter) of ~ 1 μ m. The laser power was kept below 3 mW to avoid damage to the samples due to laser heating.

We have performed density-functional calculations using the projector augmented wave method (PAW) by Blöchl,¹⁸ implemented by Kresse and Joubert in the Vienna *ab initio* simulation package (VASP)¹⁹ within the Perdew-Burke-Ernzerhof (PBE) generalized gradient approximation (GGA).²⁰ The Gaussian method with a 0.1 eV width of smearing is used, along with a plane-wave cut-off energy of 500 eV and convergence criteria of 10⁻⁵ meV for the total energy calculations and 10⁻² meV for structural optimization. An automatic *k*-mesh generation method is used for the Brillouin zone integration. Some results are obtained using the MedeA[®] software environment.²¹ The atomic forces were calculated with VASP using Hellmann-Feynman theorem with kinetic energy cutoff of 500 eV.

We study supercells of graphene with concentrations of nitrogen impurity from 0.3% to 2.0%. Here, the dopant concentration (%) indicates the number of N atoms per carbon atom. In each cell, one carbon atom is replaced with the nitrogen atom, and the structure is fully relaxed. These calculations are used to estimate the effect of the nitrogen impurity on the N-C bond length. Fig. 1 schematically shows the structure used in our calculations. In each of these cells, there is one N-atom and $n - 1$ C-atoms; thus, the size of the cell directly determines percentage of nitrogen impurity. Translational symmetry is imposed in all calculations. The initial interatomic distance is set to the C-C bond length distance of bulk graphite of 0.142 nm. It is confirmed that the impurity N-atom and its nearest neighbor C-atoms remain in-plane, i.e., within the precision of our calculations, they have negligible out-of-plane component after the structure is optimized, consistent with earlier reports, including our own experimental results.^{8,11}

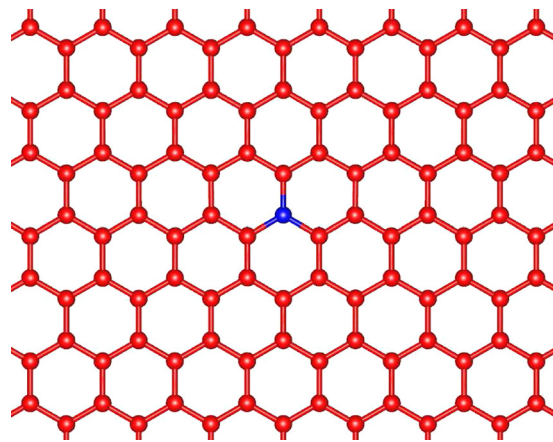


FIG. 1. Geometry of the N-doped graphene used in the calculations. Red indicates carbon, and blue indicates nitrogen.

Raman mapping was conducted over N-doped graphene samples with multiple doping levels which were transferred on to SiO₂/Si substrates. The N concentration for each sample was determined by X-ray absorption (XAS) and emission (XES) spectroscopy.²² A typical Raman spectrum for N-doped graphene (0.68%) is displayed in Fig. 2(a). A spectrum from pristine graphene (0.0% N concentration) is included for comparison. The spectrum from pristine graphene shows well-defined G and 2D bands and a negligible D band, indicating that the quality of the sample is very high. In addition to the G and 2D bands, D and D' peaks that are associated with the presence of N dopants in the graphene lattice are clearly seen in the spectrum from N-doped graphene. In order to account for the spatial inhomogeneity of the N concentration, we conducted scanning Raman microscopy with a scanning step size of 1 μ m over an area of 80 \times 80 μ m² on each sample surface that we probed. We further performed statistical analysis of these 6400 Raman spectra for each sample. Figure 2(b) shows the histograms of G peak frequency distributions obtained from pristine graphene (0.0%) and N-doped graphene with four increasing N concentrations. The red vertical dashed lines highlight the frequencies at which maximum occurrences occur. The G-peak frequency (with the maximum occurrence) versus the N-doping concentration is summarized in Fig. 2(c). Each data point in Fig. 2(c) represents the average of 6400 independent measurements to minimize statistical uncertainty. It is seen that the G peak first softens for low N-doping concentrations and then hardens for higher doping levels (in comparison to the G-frequency of the pristine graphene). This non-monotonic change of G frequency as a function of doping level is in contrast with the monotonic upshift of G frequency as a function of charge carrier concentration in electrically gated single layer graphene.^{23,24}

The nitrogen doping of graphene could lead to changes in local bonding environment, as well as Friedel type charge oscillations. Below we describe these phenomena and their possible relation with the change of G-mode frequency. Doping of graphene with nitrogen may also create localized states. Earlier studies of the doped graphene showed that this results in Friedel oscillations of the charge density, and consequently in oscillatory behavior of the localized densities of states (DOS) around the impurity site.^{25,26} Such charge

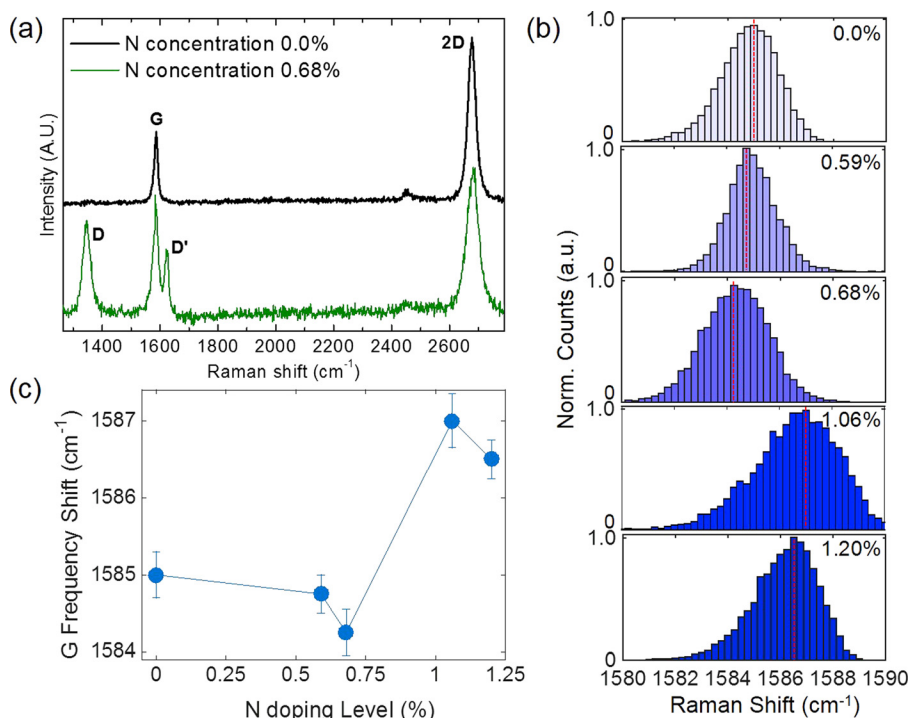


FIG. 2. (a) Typical Raman spectra from pristine graphene (0.0%) and from the sample with N concentration of 0.68%. (b) Distributions of G Raman peak frequencies for pristine graphene (0.0%) and N-doped graphene with four different N concentrations. Each distribution was obtained from 6400 points in Raman mapping. The red vertical lines highlight the frequencies that have the maximum occurrences. (c) G peak frequency as a function of N dopant concentration. The error bars are estimated as the bin size in the histograms in Fig. 2(b), so they are mainly related to the film spatial inhomogeneity. The number of independent doping concentrations we are able to study is limited by process variability and sample inhomogeneity.

oscillations could be at least in part responsible for the observed phonon frequency behavior. To test this assumption, we calculated distribution of impurity induced charge in a series of 50, 72, 98, 128, 162, 200, 242, 288, 338, and 392 atom supercells of graphene, with one of the carbon atoms being replaced with nitrogen.

In Fig. 3, we plot the charge integrated in the atomic sphere on the impurity nitrogen atom as a function of N-concentration (Fig. 3(a)), and the charge on the carbon atoms neighboring the impurity site (Fig. 3(b)) as a function of distance from the nitrogen atom in three of the considered supercells. The latter clearly indicates Friedel like charge oscillations around the impurity site which die out at around the fifth nearest neighbor carbon atom. At the same time, our calculations indicate that these charge oscillations on carbon atoms are essentially independent of doping concentration, and, within the precision of our calculations, all considered supercells produced the same distribution of oscillations. Thus, we conclude that the presence of Friedel oscillation alone would be insufficient to produce the doping dependent G-mode frequency change in graphene.

The strong dependence of the charge integrated in the atomic sphere (“effective charge”) on the impurity nitrogen atom on the concentration of N impurity (Fig. 3(a)) is due to

the long-range interaction between the delocalized defect states that lie at the Fermi level.^{8,27} These states interact with each other in the supercell, leading to rather irregular charge occupancy at the given site. The oscillation dies out as the concentration decreases (i.e., the size of the supercell increases), and when concentration is less than 0.3%, the integrated charge around the nitrogen defect site is more or less constant (Fig. 3(a)). This suggests that when defect concentrations are more than 0.3%, one needs to consider effects beyond isolated impurity to take into account the shift of the G-mode.

In addition, the doping of nitrogen affects local bonding. First, the N-C bond (1.40 Å) is shorter than the C-C bond (1.42 Å); second, also due to different “effective charge,” the bond length is expected to fluctuate as a function of the doping concentrations. In Fig. 4, we plot the N-C bond length as a function of the N-concentration. As can be seen from the plot, the bond length is irregular, similar to the plot of “effective charge” as a function of the doping. The larger effective charge leads to stronger bonding and the shorter bond length. The effect of N-doping does not extend beyond immediate neighbor. Shortening of the bond additionally adds to the stiffening of the phonons. In fact, in the past, the bond shortening has been attributed to the G-mode frequency shift.^{28,29} In particular, it has been reported that the Raman

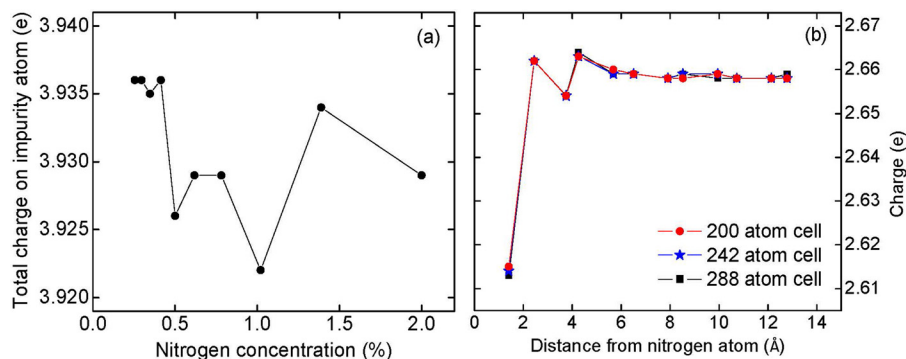


FIG. 3. (a) Charge on impurity atoms as a function on N-concentration; (b) Friedel charge oscillations: charge on the carbon atoms neighboring nitrogen impurity, as a function of distance from nitrogen atom.

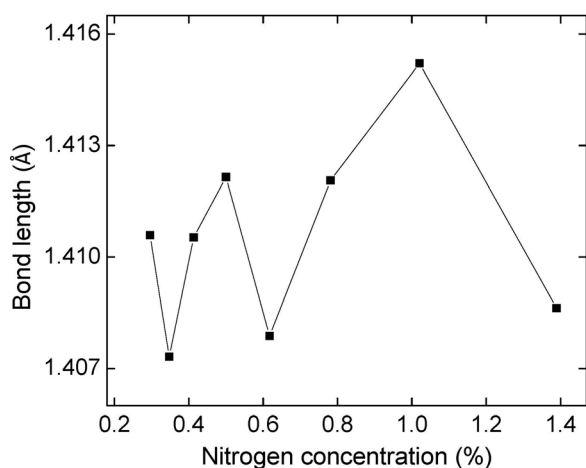


FIG. 4. Bond length between N-atom and its nearest neighbor C-atom as a function of nitrogen concentration.

shift in graphene evolves under external pressure.³⁰ Application of pressure (compressive strain) increases the value of the G-peak of the vibrational in-plane frequencies.^{31,32} The effect was observed both experimentally and confirmed theoretically by calculating the pressure-induced shift of the G-peak using the Grüneisen parameter for graphene.^{31,33} It was also showed that this effect is similar for both free standing and supported samples of graphene and holds for a wide range of the applied pressure (up to 8 GPa).³³

Based on the arguments presented above, it is plausible to propose that there is a combination of different physical phenomena, such as long-range interactions of the nitrogen point defects, and the bond length change between nitrogen impurity and its nearest neighbor carbon atoms, which contribute to the observed G phonon frequency oscillations. Decoupling of these contributions may require high precision phonon frequency calculations for smaller N-concentrations (larger cells), and goes beyond the scope of this paper. We envision this as an interesting subject of future research.

In conclusion, we studied the behavior of the G phonon frequency in the nitrogen doped graphene as a function of N-concentration. We showed that this dependence is irregular, somewhat resembling an oscillatory behavior. Our calculations indicate that these oscillations are likely to be due to the combination of different physical mechanisms, such as long-range interactions of the nitrogen point defects, and the bond length change between nitrogen impurity and its nearest neighbor carbon atoms. At the same time, we showed that impurity induced Friedel charge oscillations are unlikely to contribute to this behavior. We hope that these results provide insights on phonon frequencies in graphene as a function of impurity concentration.

This work was supported by the National Science Foundation (NSF) through the summer programs of the Nebraska Materials Research Science and Engineering Center (Grant No. DMR-1420645). R.H. acknowledges the support of the American Chemical Society Petroleum Research Fund (Grant No. 53401-UNI10) and the NSF (Grant No. DMR-1410496). P.V.L. acknowledges the support of the UNI Faculty Summer Fellowship. Computations were performed at the University of Nebraska Holland Computing Center and at

the computer facilities of the University of Northern Iowa (UNI). Synchrotron measurements performed by TS to determine the atomic concentration of nitrogen were supported by the NSF MRSEC program through Columbia in the Center for Precision Assembly of Superstratic and Superatomic Solids (DMR-1420634).

- ¹D. L. Nika, E. P. Pokatilov, A. S. Askerov, and A. A. Balandin, *Phys. Rev. B* **79**, 155413 (2009).
- ²A. Balandin, *Nat. Mater.* **10**, 569–581 (2011).
- ³I. W. Frank, D. M. Tanenbaum, A. M. van der Zande, and P. L. McEuen, *J. Vac. Sci. Technol. B* **25**, 2558 (2007).
- ⁴F. Hao, D. Fang, and Z. Xu, *Appl. Phys. Lett.* **99**, 041901 (2011).
- ⁵I. N. Kholmanov, C. W. Magnuson, A. E. Aliev, H. Li, B. Zhang, J. W. Suk, L. Zhang, E. Peng, S. H. Mousavi, A. B. Khanikaev, R. Piner, G. Shvets, and R. S. Ruoff, *Nano Lett.* **12**(11), 5679–5683 (2012).
- ⁶P. Blake, P. D. Brimicombe, R. R. Nair, T. J. Booth, D. Jiang, F. Schedin, L. A. Ponomarenko, S. V. Morozov, H. F. Gleeson, E. W. Hill, A. K. Geim, and K. S. Novoselov, *Nano Lett.* **8**(6), 1704 (2008).
- ⁷D. Wei, Y. Liu, Y. Wang, H. Zhang, L. Huang, and G. Yu, *Nano Lett.* **9**(5), 1752 (2009).
- ⁸B. Zheng, P. Hermet, and L. Henrard, *ACS Nano* **4**(7), 4165 (2010).
- ⁹Z. Jin, J. Yao, C. Kittrell, and J. M. Tour, *ACS Nano* **5**(5), 4112 (2011).
- ¹⁰L. Zhao, R. He, A. Zabet-Khosousi, K. S. Kim, T. Schiros, M. Roth, P. Kim, G. W. Flynn, A. Pinczuk, and A. N. Pasupathy, *Nano Lett.* **15**(2), 1428–1436 (2015).
- ¹¹L. Zhao, R. He, K. T. Rim, T. Schiros, K. S. Kim, H. Zhou, C. Gutiérrez, S. P. Chockalingam, C. J. Arguello, L. Pálová, D. Nordlund, M. S. Hybertsen, D. R. Reichman, T. F. Heinz, P. Kim, A. Pinczuk, G. W. Flynn, and A. N. Pasupathy, *Science* **333**, 999 (2011).
- ¹²X. Wang, X. Li, L. Zhang, Y. Yoon, P. K. Weber, H. Wang, J. Guo, and H. Dai, *Science* **324**, 768 (2009).
- ¹³B. Guo, Q. Liu, E. Chen, H. Zhu, L. Fang, and J. R. Gong, *Nano Lett.* **10**, 4975 (2010).
- ¹⁴C. Zhang, L. Fu, N. Liu, M. Liu, Y. Wang, and Z. Liu, *Adv. Mater.* **23**, 1020 (2011).
- ¹⁵A. L. M. Reddy, A. Srivastava, S. R. Gowda, H. Gullapalli, M. Dubey, and P. M. Ajayan, *ACS Nano* **4**, 6337 (2010).
- ¹⁶H. Lu, A. Lipatov, S. Ryu, D. J. Kim, H. Lee, M. Y. Zhuravlev, C. B. Eom, E. Y. Tsybmal, A. Sinitkii, and A. Gruverman, *Nat. Commun.* **5**, 5518 (2014).
- ¹⁷R. Lv, Q. Li, A. R. Botello-Méndez, T. Hayashi, B. Wang, A. Berkdemir, Q. Hao, A. L. Elías, R. Cruz-Silva, H. R. Gutiérrez, Y. A. Kim, H. Muramatsu, J. Zhu, M. Endo, H. Terrones, J.-C. Charlier, M. Pan, and M. Terrones, *Sci. Rep.* **2**, 586 (2012).
- ¹⁸P. Blöchl, *Phys. Rev. B* **50**, 17953 (1994).
- ¹⁹G. Kresse and D. Joubert, *Phys. Rev. B* **59**, 1758 (1999).
- ²⁰J. P. Perdew, K. Burke, and M. Ernzerhof, *Phys. Rev. Lett.* **77**, 3865 (1996).
- ²¹MedeA[®] Version 2.16. MedeA[®] is a registered trademark of Materials Design, Inc. Angel Fire, New Mexico, USA.
- ²²T. Schiros, D. Nordlund, L. Pálová, D. Prezzi, L. Zhao, K. S. Kim, U. Wurstbauer, C. Gutiérrez, D. Delongchamp, C. Jaye, D. Fischer, H. Ogasawara, L. G. M. Pettersson, D. R. Reichman, P. Kim, M. S. Hybertsen, and A. N. Pasupathy, *Nano Lett.* **12**(8), 4025 (2012).
- ²³J. Yan, Y. Zhang, P. Kim, and A. Pinczuk, *Phys. Rev. Lett.* **98**, 166802 (2007).
- ²⁴A. Das, S. Pisana, B. Chakraborty, S. Piscanec, S. K. Saha, U. V. Waghmare, K. S. Novoselov, H. R. Krishnamurthy, A. K. Geim, A. C. Ferrari, and A. K. Sood, *Nat. Nanotechnol.* **3**, 210–215 (2008).
- ²⁵Á. Bácsi and A. Virosztek, *Phys. Rev. B* **82**, 193405 (2010).
- ²⁶J. A. Lawlor, S. R. Power, and M. S. Ferreira, *Phys. Rev. B* **88**, 205416 (2013).
- ²⁷Ph. Lambin, H. Amara, F. Ducastelle, and L. Henrard, *Phys. Rev. B* **86**, 045448 (2012).
- ²⁸M. S. Dresselhaus and P. C. Eklund, *Adv. Phys.* **49**, 705 (2000).
- ²⁹Q.-H. Yang, P.-X. Hou, M. Unno, S. Yamauchi, R. Saito, and T. Kyotani, *Nano Lett.* **5**(12), 2465–2469 (2005).
- ³⁰C. Thomsen, S. Reich, and P. Ordejón, *Phys. Rev. B* **65**, 073403 (2002).
- ³¹J. E. Proctor, E. Gregoryanz, K. S. Novoselov, M. Lotya, J. N. Coleman, and M. P. Halsall, *Phys. Rev. B* **80**, 073408 (2009).
- ³²R. He, L. Zhao, N. Petrone, K. S. Kim, M. Roth, J. Hone, P. Kim, A. Pasupathy, and A. Pinczuk, *Nano Lett.* **12**(5), 2408–2413 (2012).
- ³³T. M. G. Mohiuddin, A. Lombardo, R. R. Nair, A. Bonetti, G. Savini, R. Jalil, N. Bonini, D. M. Basko, C. Galiotis, N. Marzari, K. S. Novoselov, A. K. Geim, and A. C. Ferrari, *Phys. Rev. B* **79**, 205433 (2009).